New Energy Materials and Devices
https://www.sciltp.com/journals/nemd

Review

Advances in Lithium Compensation

Mengyan Cao [1,2,*], Shigang Ling [1,2], Yafei Liu [1,2], Zhaoxiang Wang [3,4,5,*] and Liquan Chen [3]

[1] Beijing Easpring Material Technology Co. Ltd., Beijing 100160, China
[2] Beijing General Research Institute of Mining & Metallurgy, Beijing 100160, China
[3] Beijing National Laboratory for Condensed Matter Physics, Institute of Physics, Chinese Academy of Sciences, Beijing 100190, China
[4] College of Materials Science and Opto-Electronic Technology, University of Chinese Academy of Sciences, Beijing 100190, China
[5] School of Physical Sciences, University of Chinese Academy of Sciences, Beijing 100190, China
* Correspondence: caomengyan@easpring.com (M.C.); zxwang@iphy.ac.cn (Z.W.)

How To Cite: Cao, M.; Ling, S.; Liu, Y.; et al. Advances in Lithium Compensation. *New Energy Materials and Devices* **2026**, *1*(1), 55–74.

Received: 7 June 2026
Revised: 4 July 2026
Accepted: 23 July 2026
Published: 10 August 2026

Abstract: Electrode materials with high specific capacities have attracted growing interest to meet the ever-increasing demands for high-energy-density secondary batteries. However, lithium is inevitably consumed during cycling due to various side reactions as well as formation of solid electrolyte interphases in the first few cycles. Therefore, lithium compensation is of significance in enhancing the energy density of a battery and prolonging its cycle life. This review summarizes the research advances in lithium compensation before presenting some of our own efforts in developing new strategies and exploring new mechanisms in electrochemical and chemical prelithiation. Finally, prospects are made for future research of lithium compensation strategies.

Keywords: Li-ion batteries; lithium compensation; electrochemical prelithiation; sacrificial additive; chemical prelithiation

1. Introduction

The rechargeable lithium-ion batteries (LIBs) have received extensive attention as efficient and clean energy storage devices. With the advances in consumer electronics, electric vehicles (EVs), and distributed grids, demands are rapidly growing for high-energy-density LIBs with prolonged lifetime. Therefore, lots of work has been conducted on developing the electrode materials to improve the gravimetric or volumetric energy density of the battery [1–3].

Various high-capacity electrode materials (e.g., those by alloying reactions [4] and by conversion reactions [5]) have been used as the anode materials for next-generation LIBs. However, massive lithium ions are consumed on these materials due to the formation of the solid electrolyte interphase (SEI) in the initial cycles and the continuous lithium loss in side reactions of the electrolyte and due to lattice disintegration of the electrode. In order to address these issues and make better use of these high-capacity electrode materials, strategies have been proposed to mitigate the loss of lithium, such as construction of artificial SEI layers [6] and introduction of surface protection coatings [7]. Although some advances have been made, the way towards higher energy-density LIBs is still long.

Lithium compensation has emerged as one of the most promising strategies to replenish the lost Li and alleviate the fading of energy density. This concept had been extensively explored in lithium-ion capacitors before its broader application in LIB, mainly to lower the anode potential, compensate for the irreversibly consumed Li, and extend the operating voltage window [8]. Since 2010, the lithium compensation has been growing exponentially in LIB research [9]. The lithium compensation techniques can be viewed as providing additional lithium in the cathode, anode, or separator [10–12]. Herein, we review the advances of lithium compensation strategies and their challenges. After a brief review of the research advances in the field, we showed some of our

recent work in electrochemical and chemical prelithiation. A prospect was made at the end of this review, presenting some insights or future directions of lithium compensation to stimulate more inspiration.

2. Recent Research Advances

Various lithium compensation strategies have been developed. In this review, depending on the driving force for the lithium compensation, we divide these strategies into electrochemical compensation or chemical prelithiation. Of course, lithium ions can be introduced into the electrode material before (prelithiation in powder of the active material or in electrode sheet) or after (with pre-loaded sacrificial Li-rich additives) battery assembly.

2.1. Electrochemical Compensation

Electrochemical compensation refers to the process of lithium transfer from a metallic lithium electrode or a Li-rich additive-containing electrode to the target electrode in an electrochemical cell [13]. In these approaches, the number of prelithiated Li-ions can be controlled by regulating the current and time, the cut-off voltage, as well as the additive loading.

2.1.1. Compensation from Metallic Lithium (Li^0)

The Li^0-mediated prelithiation refers to a prelithiation process in which the metallic lithium (Li^0) electrode serves as the lithium reservoir and the Li-ion is transferred into the target electrode under a controlled external voltage. This approach has been widely applied in prelithiating both the cathode materials (polyanions such as $Li_3V_2(PO_4)_3$ [14] and $LiVPO_4F$ [15], layer-structured such as $LiNi_{0.5}Mn_{0.3}Co_{0.2}O_2$ (LNMCO) [16], and spinel oxides such as $LiMn_{1.5}Ni_{0.5}O_4$ [17] and $LiMn_2O_4$ [18]) and anode materials (graphite (Gr) [19–22], Si [23–25], Si/C composite [26], Ge [27], SnO_2 [28], Fe_2O_3 [29,30], Fe_3O_4 [31], MnO_x [32], and $ZnFe_2O_4$ [33]).

Si is a typical high-capacity anode material. However, a cell with a Si anode suffers from substantial loss of lithium and unstable interfacial chemistry. Li et al. [34] pre-discharged 746.6 mAh g^{-1} of Li to Si prior to the usual discharge by ex situ electrochemical prelithiation (Figure 1a); the number of the pre-inserted Li-ion was determined by measuring the irreversible capacity of pristine Si. Beneficial from the pre-stored Li and pre-generated LiF- and Li_4SiO_4-rich interphase, the Si||LNMCO cell with the prelithiated Si anode shows an initial Coulombic efficiency (ICE) of 84.7% (Figure 1b). Meanwhile, the capacity retention of the cell increases from 20.5% in the Si||LNMCO cell to 73.1% in the Li-added Si||LNMCO cell after 300 cycles.

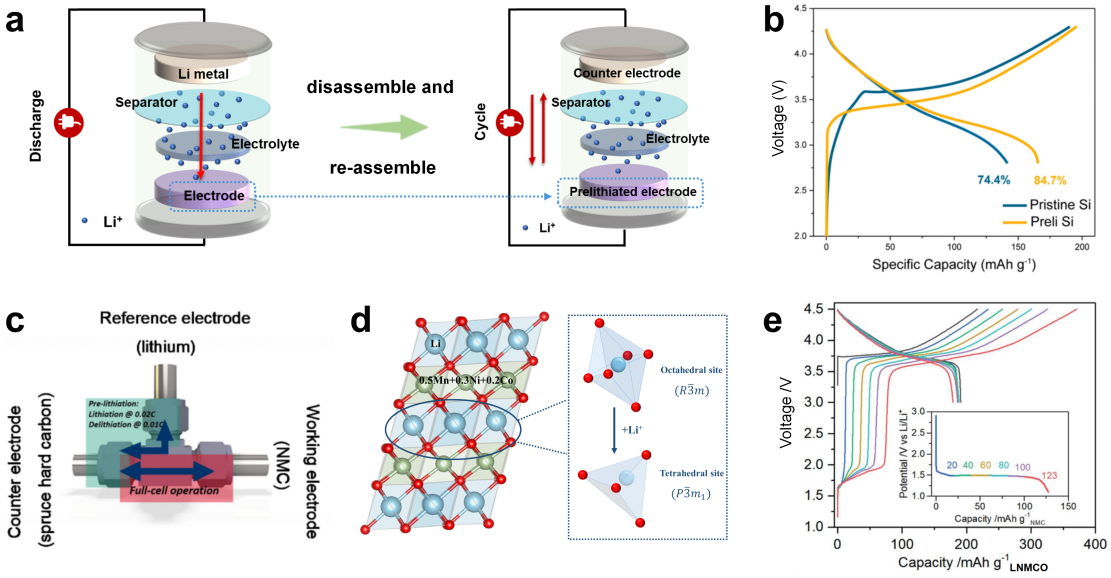

Figure 1. (**a**) Schematic diagram of ex situ Li^0-mediated prelithiation. (**b**) Comparison of the electrochemical performance of a Si||LNMCO full cell with/without prelithiation in Si [34]. Reprinted with permission from Ref. [34]. 2024, Li et al. (**c**) Schematic illustration of the in situ electrochemical prelithiation in a three-electrode cell [35]. Reprinted with permission from Ref. [35]. 2021, Drews et al. (**d**) Structural diagram and (**e**) electrochemical prelithiation performance of LNMCO [16]. Reprinted with permission from Ref. [16]. 2021, Dose et al.

In comparison to the two-electrode ex situ prelithiation that requires cell disassembly and reassembly, a three-electrode cell (Figure 1c) enables in situ prelithiation while preserving the as-formed interphase and minimizing the uncontrolled loss of Li. Drews et al. [35] employed a three-electrode Swagelok cell to prelithiate hard carbon, in which the Li metal (the third electrode) serves as the Li donor, whereas hard carbon and $LiNi_{0.33}Mn_{0.33}Co_{0.33}O_2$ (NMC) function as the other two electrodes (working electrodes) of the full cell. The hard carbon was discharged to 0.0 V (prelithiation; about 200 mAh g^{-1} of Li^+ was inserted) before it was recharged to 1.0 V. Then, the prelithiated hard carbon anode was incorporated with NMC cathode into a full cell for the subsequent cycling. The initial discharge capacity of the full cell increased from 275 mAh g^{-1} in a hard carbon||NMC cell to 295 mAh g^{-1} in a similar cell using the above prelithiated hard carbon, where the capacity was calculated based on the mass of hard carbon material.

As the structural stability of the cathode material is sensitive to its lithiation state, galvanostatic discharging can also be adopted to prelithiate the cathode materials. LNMCO is a conventional layered cathode material with the α-$NaFeO_2$ structure [36], in which the additional Li-ions occupy the octahedral sites (Figure 1d). Dose et al. [16] obtained Li_{1+x}NMCO ($0 < x < 0.5$) by discharging the Li||LNMCO half cell to different depths (Figure 1e). Over-lithiation degrades the electrochemical performance (the red galvanostatic profile in Figure 1e). Therefore, low-to-medium prelithiation is recommended. Optimized prelithiation (Li insertion capacity of 20~70 mAh g^{-1}) allows LNMCO to deliver both a higher reversible capacity in the initial charge and a superior capacity retention in 100 cycles (increase from 59% to 62%~89%). Similarly, $Li_3V_2(PO_4)_3$, a monoclinic polyanionic material with an open three-dimensional framework, can accommodate two additional Li ions upon galvanostatic discharge to form $Li_5V_2(PO_4)_3$ [14]. Upon full-cell assembly with hard carbon, $Li_5V_2(PO_4)_3$ exhibits an improved initial reversible capacity from 82.1 to 124.2 mAh g^{-1}.

Although the electrochemical (especially galvanostatic) prelithiation enables precise control of the prelithiation amount, it is achieved at the expense of prelithiation efficiency and manufacturing facility. Kim et al. [25] proposed prelithiation by monitoring/controlling the cut-off voltage of the cell, in which the target electrode (to be prelithiated) is connected to metallic Li by an external circuit. Owing to its inaccuracy of prelithiation, this strategy is suitable for anode materials that are insensitive to over-prelithiation (lithium dendrites cannot be formed above 0.0 V due to polarization effects and overpotential for Li nucleation), such as Gr [21,22] and SiO_x [25].

Overall, galvanostatic prelithiation is characteristic of high controllability, making it suitable for mechanistic studies and evaluation of the optimal prelithiation amount. In some cases, prelithiation is finished in more than one cycles; controlled lithiation-delithiation pretreatment is conducted in each cycle in order to pre-form and stabilize the anode interphase [37].

2.1.2. Li-Rich Compounds for Prelithiation

The advantage of the metallic-lithium-mediated prelithiation lies in providing a clean Li source. It enables Li insertion without residues that interfere with the mechanistic analysis. However, it is incompatible to the practical battery manufacturing: use of metallic Li either requires an additional electrode (as Li source) and lowers the practical energy density, or necessitates later separation of prelithiated electrode, which increases processing complexity and reduces production efficiency.

In comparison, electrochemical prelithiation from the Li-rich compounds (additives) offers a more attractive combination of controllability and practical applicability. It generally relies on Li-rich compounds that undergo (nearly) irreversible delithiation in the initial cycle, thereby releasing Li-ions to compensate for Li loss. An ideal additive should meet some requirements, including (1) high theoretical specific capacity to provide effective Li compensation with a limited addition content; (2) favorable delithiation products and compatibility with the electrode materials and battery; and (3) high chemical and air stability. Given their distinct characteristics, such additives can be introduced in the cathode side, anode side, or on the separator.

Li-Rich Additives in Cathode

In addition to the above requirements, the cathode-side Li-rich additives are further expected to have some specific features. (1) Appropriate delithiation potential: the delithiation potential should be located below the charge cut-off voltage of the cell or not too high above it to ensure sufficient Li release without destructing the cathode material or electrolyte. (2) Controlled loading: the additive loading should be balanced to ensure effective Li compensation while preventing over-lithiation of the anode material (e.g., Li plating or structural degradation) or the cathode itself (it is very possible that the lithium from an over-lithiated anode will over-lithiate the cathode in the subsequent charging for a battery with a normal N/P capacity ratio). Such Li-inventory mismatch may further raise safety concerns during formation and cycling. (3) Facile processing and high chemical compatibility to the

cathode: the additive should be compatible to the slurry processing of the cathode, with moderate alkalinity to avoid detrimental effects on the binder, and should not induce in situ reduction of the cathode material before electrochemical activation. (4) High thermal stability: the additive and its delithiated residues should possess high thermal stability, as reactive surfaces or residual species may accelerate electrolyte decomposition and heat/gas generation at elevated temperatures.

A variety of cathode Li-rich additives have been reported, such as Li_2O [38,39], Li_2O_2 [40,41], Li_3N [42,43], Li_2CO_3 [44], LiF [45,46], Li_5FeO_4 [47–49], Li_6CoO_4 [50–52], $Li_xC_6O_6$ [53], Li_4SiO_4 [54], etc. Nevertheless, each material suffers from some intrinsic limitations.

(1) Excessively high delithiation potentials. The delithiation potential of some proposed additives is usually far above the practical operation voltage window of the cathode materials, resulting in incomplete delithiation and insufficient Li donation, which compromises the actual Li compensation efficiency, such as Li_2O [38,39], Li_2O_2 [40,41], LiF [45,46], $Li_2C_2O_4$ [55–59], Li_4SiO_4 [54], and Li_2CO_3 [44]. In order to break up this limitation, current efforts mainly focus on reducing the particle size [55], constructing the conductive carbon networks [60], and introducing catalysts [59] to lower the overpotential and facilitate the activation process. Catalyst was introduced to promote the delithiation reaction or regulate the delithiation pathway of the Li_2CO_3- and Li_2O-based additives. Doping of Co and introduction of Li defects decrease bandgap and weaken the Li-O interaction of Li_2CO_3 (Figure 2a), lowering its delithiation potential from above 4.6 V to around 4.4 V (Figure 2b). In addition, transition-metal incorporation was also applied to modify the delithiation pathway rather than merely accelerate the reaction kinetics [39]. Sun et al. [39] prepared nanocomposite of Li_2O and metallic Co by reducing Co_3O_4 with molten metallic Li ($Co_3O_4 + 8Li \rightarrow 4Li_2O + 3Co$) and used the nanocomposite (Li_2O/Co) as Li-compensation additive on the cathode. The presence of Co nanoparticles in the nanocomposite transforms the conventional direct delithiation of Li_2O ($2Li_2O \rightarrow 4Li^+ + 4e^- + O_2$) into a new conversion reaction ($4Li_2O + 3Co \rightarrow Co_3O_4 + 8Li^+ + 8e^-$). Meanwhile, the delithiation potential of Li_2O was reduced to below 4.0 V. Similar strategies can be used to prepare nanocomposites of Li_2O/Fe and Li_2O/Ni additives. However, the dissolution of the Co/Fe/Ni metal nanoparticles and their oxides in the electrolyte might arise safety concerns in practical cells.

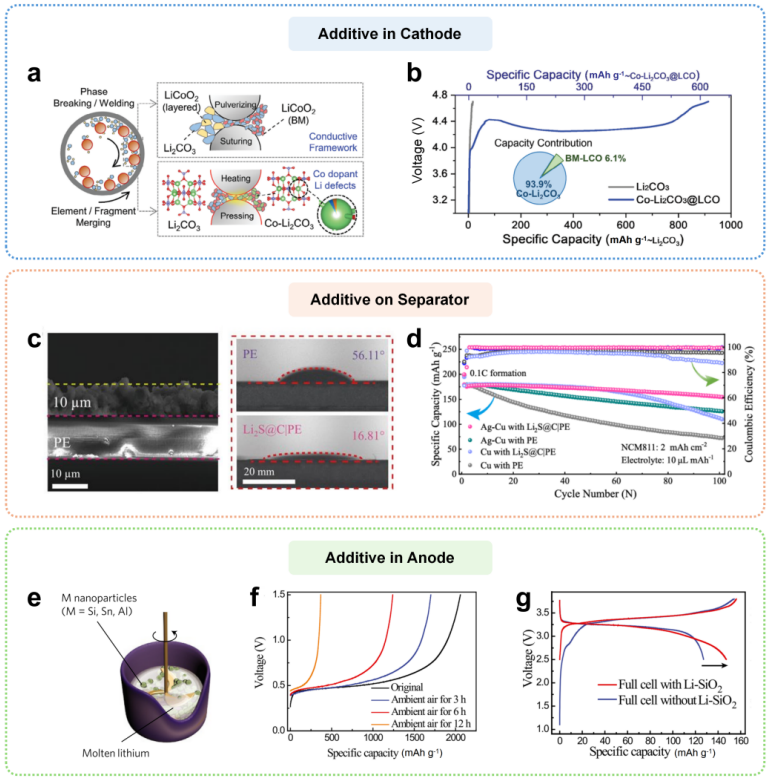

Figure 2. (**a**,**b**) Improvement strategies and electrochemical performance of Li_2CO_3 additive [44]. Reprinted with permission from Ref. [44]. 2023, Zhu et al. (**c**) The cross-section image of the Li_2S@C functional separator and the contact angles of the electrolyte drop on the Li_2S@C|polyolefin (PE) and PE separators. (**d**) The cyclability of different cell configurations with PE and Li_2S@C|PE separator [10]. Reprinted with permission from Ref. [10]. 2025, Shao et al. (**e**) Schematic diagram of the synthesis of the Li alloy additive [61]. Reprinted with permission from Ref. [61]. 2017, Zhao et al. (**f**) The initial charge voltage profiles of Li_xSi-Li_2O composite additive and (**g**) prelithiation performance of the additive in the full cell [62]. Reprinted with permission from Ref. [62]. 2016, Zhao et al.

(2) Poor stability in air. The high alkali on the surface is one of the major concerns for the application of the Li-rich additives, such as Li_2NiO_2 [63,64], Li_3BO_3 [65], Li_3N [42,43], Li_5FeO_4 [47–49], and Li_6CoO_4 [50–52]. These additives are susceptible to parasitic reactions with ambient moisture and CO_2 during storage and electrode processing as they are highly lithiated and often possess active surfaces, leading to formation of residual Li species such as LiOH and Li_2CO_3 [48]. Such surface degradation not only consumes active Li but also deteriorates the processing stability and interfacial compatibility. Surface engineering is an effective strategy to improve the air stability of Li-rich compensation additives. In practice, the most commonly adopted protective layers are composed of carbon [48], phosphate [66], Li_2CO_3 [65], and sulfur-containing substances [52]. Liu et al. [48] utilized pitch-pyrolized carbon coating to improve the air stability of Li_5FeO_4. The Li_5FeO_4@C retained 92.3% of its initial specific capacity after exposure to air for 72 h at 20% relative humidity. This proves the effectiveness of the carbon layer in shielding the Li_5FeO_4 from external air interactions. Similarly, Liu et al. [52] stabilized Li_6CoO_4 with a conformal sulfur coating, suppressing the gas generation by chemically trapping the released oxygen and redirecting it from O_2 evolution into sulfate formation ($Li_6CoO_4 + 0.5S \rightarrow 4Li^+ + 4e^- + LiCoO_2 + 0.5Li_2SO_4$).

(3) Unfavorable delithiation products and reactive intermediates. (1) Gas evolution is typically an undesirable feature of Li compensation additives, as it can induce electrode swelling, deteriorate interfacial contact, and raise potential safety risks. Moreover, gas evolution rarely occurs alone; it is often associated with the aforementioned drawbacks. Gases are observed when Li_2O, Li_3N, and Li_6CoO_4 are applied as the additive. Gassing can be effectively mitigated by altering the delithiation reaction pathway [39] or introducing protective layers [52]. (2) Undesirable soluble products may also pose challenges to battery performance. For example, the organic additives (such as $Li_2C_4O_4$ [67,68], Li_2DHBA [69], $Li_2C_6O_6$ [53], and $Li_4C_6O_6$ [53]) leave no solid residues, but their organic products may dissolve into the electrolyte. This working mode inherently imposes strict requirements on electrolyte compatibility with the dissolved organic species. In addition to catalyzing the electrolyte, the residual solid product of the delithiated additive may be dissolved (e.g., Fe^{2+}) into the electrolyte. These dissolved Fe-species can migrate to the anode, where they facilitate continuous SEI growth and may even trigger formation of Fe dendrites, ultimately undermining the battery safety. Zhu et al. [70] employed an ultrathin C_3N_4 protective layer to inhibit Fe^{2+} dissolution. (3) In the case of Li_2S [71,72], the main challenge arises from the formation of soluble polysulfide intermediates, which can trigger shuttling behavior and parasitic reactions. Accordingly, strategies such as conductive carbon confinement [73] and Li_2S/metal nanocomposite design [71] were developed to restrain the formation and dissolution of polysulfide.

Trade-offs are still inevitable, though considerable progress has been achieved in addressing the intrinsic drawbacks of different Li-rich additives. For example, introduction of Fe metal could significantly lower the delithiation potential of LiF and Li_2O or avoid the formation of polysulfide, but the presence of metallic Fe in manufacture is undesirable; it may induce internal micro-short circuits and raise safety concerns. Surface coating can significantly enhance the air stability of Li_5FeO_4. However, both its delithiated products ($LiFeO_2$) and the coating layers are electrochemically inactive, leading to increased electrode resistance and incomplete capacity utilization.

Li-Rich Additives on Separator

Clearly, in addition to forming a uniform composite with the cathode materials, the Li-compensation agents can be loaded on the separator as well. The additive-coated separator is usually called the Li-replenishing separator (LRS). An ideal separator-based Li-compensation material should possess the following additional characteristics: (1) high dispersibility and strong film-forming or composite-forming capability to enable uniform immobilization on one side of the separator; (2) appropriate particle size and morphology to avoid particle penetration, severe surface roughening, or local pore blockage; and (3) good compatibility with separator functions, including porosity, electrolyte wettability, mechanical integrity, and Li-ion transport. Examples of Li-compensation agents include Li_2S [10,74], $Li_2C_2O_4$ [75,76], Li_5FeO_4 [77,78], $Li_2C_4O_4$ [79], and lithium 2,3,5,6-tetrafluorobenzene-1,4-bis(olate) [80]. In order to ensure the Li compensation activity and compatibility with the separator, these additives have to be composited with carbon materials or other catalysts. Shao et al. [10] integrated a Li_2S@C layer (~10 μm thick) onto a PE separator to improve the initial discharge capacity of Ag-Cu||$LiNi_{0.8}Co_{0.1}Mn_{0.1}O_2$ cell (Figure 2d) as well as to enhance its electrolyte wettability (Figure 2c).

Despite the notable progress achieved to date, transferring the sacrificial additives from the cathode to the separator can only alleviate the detrimental impact that the additives might have on the cell, but cannot eliminate the associated side reactions. In fact, prelithiation by LRS is constrained with some intrinsic limitations: an inherent trade-off between prelithiation capacity and the Li-ion transport properties of the separator (coating prelithiation additives on the separator decreases the porosity of the separator and elongates the Li-ion diffusion pathway) and the difficulty for one LRS to quantitatively match Li-ion batteries with different areal capacity loadings.

Li-Rich Additives in Anode

Similarly, an ideal anode-side Li-rich additive is supposed to possess the following features: (1) moderate Li-release reactivity and controllable release kinetics. The additive should release Li efficiently, but not so aggressively as to induce severe local side reactions or interfacial instability; (2) sufficiently high stability to accommodate practical electrode manufacturing and storage and processing compatibility to the anode system; (3) no induction of premature parasitic reactions, disrupt slurry rheology, or compromise electrode integrity prior to electrochemical activation. Of course, the additive loading should be judiciously controlled to provide sufficient Li compensation without resulting in excessive Li supply, which may over-lithiate or over-reduce the cathode material and thereby degrade its structural stability.

Lithium-silicon (Li-Si) alloys (Li_xSi) are typical anode Li-rich additives. They are generally obtained by the direct reaction of metallic Li with Si anodes (Figure 2e). Alloys from $Li_{13}Si_4$ to $Li_{22}Si_5$ theoretically deliver specific capacities of 1700 to 2100 mAh g^{-1}. However, the highly lithiated silicon is highly reactive in air and humidity. In order to mitigate this issue, Zhao et al. [81] constructed an artificial passivation layer on Li_xSi using its strong reductivity to 1-fluorodecane. The LiF- and lithium alkyl-carbonate-enriched passivation layer improved the air stability of Li_xSi while preserving its electrochemical activity. After exposure to dry air with a dew point of −50 °C for 120 h, the capacity retention of the coated Li_xSi was improved from 68% to 92%. In addition, protection with Gr foil [61], Li_2O shell [62,82], and polyethylene oxide (PEO) [83] can also effectively enhance the stability of Li_xSi. The reaction between SiO_2 and metallic Li can yield a Li_xSi/Li_2O composite, where the Li_2O phase effectively protects the highly reactive Li_xSi domains from direct exposure to air, thereby enabling both ambient-air compatibility (Figure 2f) and high prelithiation capacity (Figure 2g) [62]. Notably, the role of Li_xSi has currently been extended from independent prelithiation additives to integrated structural units within anodes. Zhang et al. [84] applied the $Li_{21}Si_5/Si\text{-}Li_{21}Si_5$ bi-layer anode for all-solid-state Si-based batteries, in which $Li_{21}Si_5$ facilitates the construction of a continuous conductive network and accommodates the volumetric variation of the anode.

The Ge- and Sn-based Li-alloys were also used as anode Li-rich additives. Zhao et al. [85] developed a one-pot metallurgical prelithiation strategy for group IV elements and their oxides, enabling the synthesis of $Li_{22}Z_5$ alloys and $Li_{22}Z_5\text{-}Li_2O$ composites (Z=Si, Ge, Sn). In these systems, the host element and the Li_2O matrix synergistically regulate the Li-compensation capability and air stability of the additives. In comparison, the Li_xSi alloys are more attractive as they provide a better balance among Li-storage capacity, material cost, resource abundance, and practical relevance to the Si/SiO_x anodes.

Despite these advances, the practical value of anode Li-rich additives is still limited due to the following penalties. Firstly, introduction of protective components, such as Li_2O matrices in Li_xSi composites, inevitably occupies electrode volume and alters the local electrode microstructure. This may reduce electrode compact density, disturb ion/electron transport pathways, and increase interfacial resistance. Moreover, once incorporated into practical thick electrodes, the Li-release behavior of Li_xSi additives becomes highly sensitive to particle dispersion, local conductive networks, electrolyte accessibility, and formation protocols, making it difficult to achieve spatially uniform and quantitatively matched lithium compensation.

2.2. Chemical Prelithiation

Chemical prelithiation refers to a process in which prelithiation is achieved through spontaneous chemical reactions between electrode materials and Li-donating reagents with chemical Li-supply capability. Depending on the reaction temperature, chemical prelithiation can generally be classified into high-temperature chemical prelithiation and chemical prelithiation around room temperature.

2.2.1. Prelithiation at High Temperatures

The high-temperature chemical prelithiation can be conducted in two ways, sintering and soaking in molten salt. Sintering prelithiation relies on the thermally driven solid-state reactions between Li-containing compounds and electrode materials at high temperature, enhancing the diffusion and incorporation of Li ions into the host lattice. Actually, most of the current Li-containing cathode materials are obtained by the solid-state sintering [86]. Moreover, sintering is also applied in Li re-insertion, regeneration of the spent cathode materials, such as $LiFePO_4$ (LFP) [87], $LiCoO_2$ [88], and $LiNi_{1/3}Co_{1/3}Mn_{1/3}O_2$ [89]. Ji et al. [87] regenerated spent LFP with 3,4-dihydroxybenzonitrile dilithium (Li_2DHBN) as a multifunctional Li precursor (Figure 3a). The thermal decomposition of Li_2DHBN at low temperatures (200–400 °C) into amorphous carbon helps to improve the conductivity of LFP, while further decomposition of ($Li_2CO_3\rightarrow$) Li_2O (at around 700 °C) provides Li for LFP regeneration. In comparison to the direct sintering of Li_2CO_3 or LiOH with spent LFP, the reductive cyano groups of Li_2DHBN suppress the formation of Fe^{3+} species in LFP (Figure 3b).

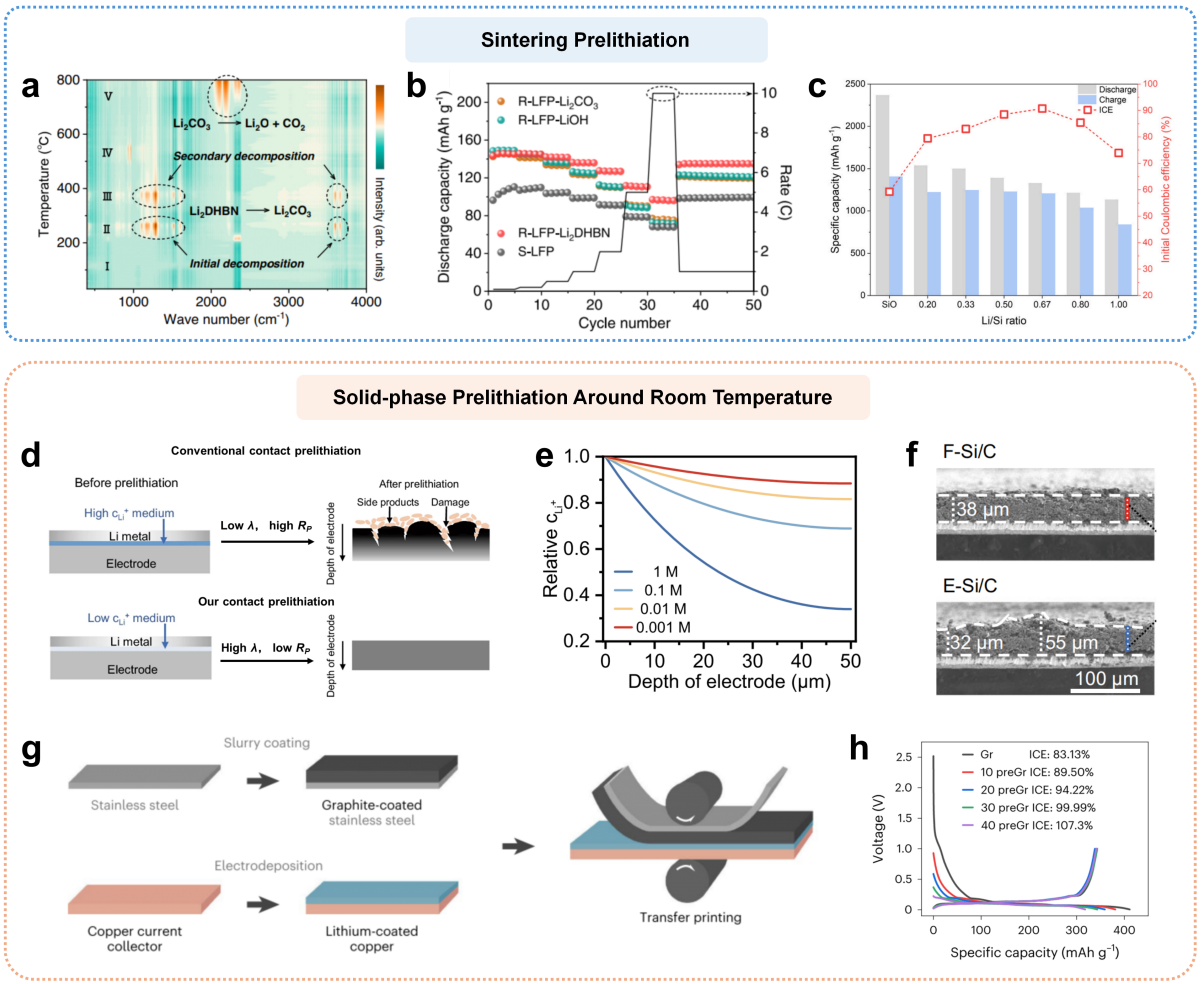

Figure 3. (**a**) Regeneration of spent LFP by pyrolysis of Li_2DHBN. (**b**) Comparison of the rate performance of spent LFP and regenerated LFP [87]. (**c**) Comparison of the specific capacity and ICE of prelithiated SiO under different conditions [90]. Reprinted with permission from Ref. [90]. 2021, Chung et al. (**d**) The impact of Li^+ concentration of the media on electrode prelithiation. (**e**) Calculated Li-ion depth distribution after prelithiation using media with different Li^+ concentrations. (**f**) The cross-sectional images of prelithiated Si/C anode using high Li^+ concentration (1 mol L^{-1} $LiPF_6$-based electrolyte, denoted with E-Si/C) and low Li^+ concentration (fluoroethylene carbonate, denoted with F-Si/C) of media [91]. (**g**) The schematic illustration of the fabrication of prelithiated Gr by "transfer-printing" methods and (**h**) the electrochemical performance of prelithiated Gr [92].

LiH is a representative reagent for sintering prelithiation in Si [93] and SiO (a composite of Si and SiO_2) [90] materials. Chung et al. [90] introduced Li through a high-temperature solid-state reaction between SiO and LiH at 750 °C. It is shown that the ICE of SiO increased with the Li/Si ratio and reached its maximum at 0.67, indicating that this ratio was the optimal prelithiation condition (Figure 3c). The detailed microstructural characterization revealed that prelithiated SiO evolved from a homogeneous amorphous matrix into a composite microstructure composed of Si-rich domains and lithium silicate phases. When incorporated into a Gr/SiO||$LiNi_{0.6}Co_{0.2}Mn_{0.2}O_2$ full cell with a Gr/SiO mass ratio of 4.3:1, the initial discharge capacity increases from 24.8 mAh to 37.0 mAh.

Molten-salt prelithiation is another important high-temperature prelithiation strategy. Li et al. [94] reported a LiCl-induced thermochemical prelithiation approach for SiO_x, in which molten LiCl serves as a Li^+-containing reaction medium at 700 °C. The molten salt promotes bulk-level lithiation of SiO_x, enabling the activation of the inert SiO_x component, and induces favorable structural reconstruction. Through the synergistic effect of molten LiCl and $LiNH_2$, the ICE of SiO_x was prominently improved from 58.7% to 88.2% [94].

High-temperature prelithiation offers the dual advantage of compensating for the Li loss and tailoring the microstructure of the electrode materials. Nevertheless, such a prelithiation rate highly relies on the temperatures, which inevitably increase energy consumption and process complexity. Moreover, the prelithiation degree is governed with coupled thermodynamic and kinetic processes.

2.2.2. Prelithiation around Room Temperature

Solid-Phase Prelithiation

In this section, solid-phase chemical prelithiation is defined as a room-temperature prelithiation process that proceeds through solid-state reactions between the electrode material and the Li-containing phase. This process is thermodynamically driven by the difference of the chemical potentials between the target electrode material and the Li source, though, external pressure or mechanical impacts are, in some cases, applied to enhance the solid-solid contact and accelerate Li transfer, by ball-milling of the powders or by compressing metallic Li (foil or powder) on the anode (material).

With an ultrahigh theoretical specific capacity of 3860 mAh g^{-1}, metallic Li is clearly the most efficient Li-compensation material, in forms of Li powder [95] and Li foil [96]. Most of the metallic Li is spontaneously dissolved and inserted into the lattice of the anode material (Gr [97], Si [98], SiO_x [99], Sn [100,101], and Al [96,102,103]) under the driving of the difference of the chemical potentials of the metallic Li and the anode material upon the electrolyte injection into the cell (some of the dissolved Li-ions are consumed to form SEI layer on the particle). In the initial discharge, the Li-ions pre-entered the anode material will be extracted, together with the Li-ions transferred from the cathode, and inserted into the cathode material.

That seems a perfect strategy of Li compensation. However, it is difficult to prepare very thin Li foil (a few micrometers; the capacity of 1 μm Li foil is ~0.206 mAh cm^{-2}) because of the presence of wrinkles, foil breakage, inhomogeneous thickness, pinholes, and impurities in the foil. Moreover, the direct contact between the Li-foil and electrode also results in random and nonuniform interfacial contact due to variations in stacking pressure and surface roughness. Therefore, Li-foil prelithiation has not been applied for mass production. In recent years, increasing efforts were devoted for optimization of the strategies. (1) Introduction of a Li-ion conductive intermediate buffer layer. The intermediate layer can effectively suppress direct contact between the Li foil and the electrode, thereby remarkably enhancing the uniformity of prelithiation. The buffer layer regulates the Li^+ transport rates and enables more uniform prelithiation. Ou et al. [91] introduced a salt-free cyclic carbonate medium between Li metal and the electrode. Utilizing its spontaneous reaction with Li metal, the generated mM-level soluble Li^+ species enable an equilibrium between the Li^+ diffusion and the intrinsic prelithiation rate (Figure 3d), thus realizing the controllable and uniform prelithiation (Figure 3e,f). (2) Optimization of the preparation process and form of Li. Replacing pure Li-foil with supported Li-foil, in which the carrier can be a copper foil [92] or carbon film [104], to improve the processability of the composite Li-foil. Yang et al. [92] developed the "transfer-printing" method by electrodepositing Li metal onto the current collector and then roll-calendering a pre-manufactured anode onto the deposited Li to realize Li transfer (Figure 3g). By tuning the calendering-induced compressive stress and the accompanying interfacial shear stress, this strategy enables efficient prelithiation. Furthermore, the ICE of Li||Gr increases from 83.1% to 107.3% by regulating the Li loading from 10% to 40% of the Gr capacity (Figure 3h). (3) Realizing more precise Li dosage by directly depositing metallic Li onto the electrode surface. For example, Chen et al. [105] and Adhitama et al. [106] found that metallic Li could be thermally evaporated onto the surface of SiO_x or Si, thereby enabling prelithiation through regulation of the deposited Li amount.

Some of the foil-mode issues can be well addressed in Li powder. Due to the higher activity of Li powder and stickiness of metallic Li, the Li particles have to be coated with some inert materials for stabilization and for dispersion upon application. Droplet emulsion technique (DET) [107] is one of the most mature routes for producing lithium metal powder. As early as 2005, Jarvis et al. [108] used stabilized Li metal powder (SLMP) to enhance the capacity of the Gr anode.

Nevertheless, SLMP suffers from several inherent drawbacks, including poor air stability, limited compatibility with conventional N-methylpyrrolidone (NMP)-based slurry processing, safety risks associated with lithium powder handling, and reduced effective capacity due to electrochemically inactive passivation layers. Kim et al. [95] introduced F^- and CO_2 during the DET process to construct a Li_2CO_3-LiF composite protective layer in order to improve the air stability of the lithium powder. This protective layer is mechanically fractured during electrode calendering, thereby exposing the highly active lithium powder. However, incomplete activation may leave residual SLMP particles, leading to delayed/nonuniform Li compensation and possible localized Li deposition during cycling [109]. Meanwhile, new binder systems, such as styrene butadiene rubber (SBR)-polyvinylidene difluoride (PVDF) [110] and n-heptane/polyisobutylene (PIB) [111], were developed to address the incompatibility of SLMP with NMP-based slurry systems. However, the dispersion uniformity and processing compatibility of current SLMP remain insufficient to meet practical manufacturing requirements. In addition, although the passivation layer renders SLMP non-pyrophoric in dry air, strict control of moisture, static electricity, and ignition sources is still required during practical processing.

Ball-milling prelithiation is a strategy by which the electrode materials and Li-containing compounds are mechanically activated and intimately mixed through ball milling, thereby enabling Li insertion. It was applied in silicon-based anodes using Li metal [112], LiF [113], and Li_2O [114] as the Li sources. Hu et al. [113] prelithiated SiO_x by ball milling it with LiF, achieving controllable Li compensation and formation of a LiF-rich SEI layer, thereby reducing loss of the active Li and improving the cycling stability. Nevertheless, the applicability of ball-milling prelithiation remains limited. When metallic Li is used as the Li source, its high ductility and adhesiveness can result in severe sticking to the milling jar and balls, resulting in nonuniform prelithiation. Even when nonmetallic Li-containing compounds are employed, the high mechanical energy required for effective mechanochemical lithiation remains difficult to implement in industrial manufacturing.

Despite the above significant progress, solid-state chemical prelithiation still faces several key challenges. (1) Insufficient depth-uniformity compatibility: Especially in the thick and high-loading electrodes, Li-foil prelithiation tends to induce localized Li^+ transport and reaction, thereby leading to an inhomogeneous Li distribution along the electrode thickness. (2) Strict environmental requirements and severe safety hazards: the presence of metallic lithium requires extremely stringent environmental-control requirements and inevitably raises serious safety concerns, both of which pose challenges to the cost of battery manufacturing.

Liquid-Phase Prelithiation

In view of the limitations of the above prelithiation, increasing efforts were directed toward identifying solutions with stronger reductivity, capable of prelithiation at room temperature. As early as 1999, Garcia et al. [115] reported prelithiation of V_2O_5 in an n-butyllithium-hexane solution. Lithium-liquid ammonia [116] and lithium-pentanol [117] systems were later developed. However, these systems suffer from evident drawbacks such as very narrow low-temperature windows (lithium-liquid ammonia requires strictly low-temperature conditions, typically around −78 °C) or H_2 evolution (lithium-pentanol).

In contrast, the lithium-aromatic compound complex solutions (LACSs) can effectively overcome the above limitations. The LACSs are typically prepared by reaction of metallic lithium with aromatic compounds in ether-based solvents. The structural feature of these aromatic ligands is their conjugated π-electron framework, in which the delocalized π-electron cloud provides strong electron-donating capability and enables the formation of Li-coordinated complexes through Li^+-π interactions [118]. Assisted with the solvent coordination, the resulting LACSs contain abundant radical species and exhibit pronounced reducing activity. Upon contact with an electrode material, the chemical-potential difference between the LACS and the host drives the directional transfer and insertion of Li ions into the electrode material.

A number of LACSs have been reported, including 9,9-dimethylfluorene lithium [119], naphthalene lithium (Naph-Li) [120], biphenyl lithium (Bp-Li) [121], and its derivatives [122], dissolved in chemically stable solvents such as dimethoxy ethane (DME) [123], tetrahydrofuran (THF) [124], and 2-methyl tetrahydrofuran (mTHF) [125]. These LACSs demonstrate broad applicability to both the anode and cathode materials. Taking the Naph-Li-DME solution, for example, controllable prelithiation was achieved in hard carbon by immersing the electrode in the solution, with the prelithiation degree regulated by parameters such as immersion time and solution concentration. After prelithiation, the ICE of hard carbon increases from 74% to above 100% [120]. Prelithiation with Naph-Li-THF solution increased the initial charge capacity of $LiCoO_2$ as a cathode material [124].

Although a wide variety of LACSs have been developed and exhibit markedly different reductivities (Figure 4a), their practical application is still constrained with issues such as insufficient reducing power in some systems and side reactions such as solvent co-intercalation. Jang et al. [122] investigated the effects of the type and number of substituents on the reducing capability of LACSs (Figure 4b). Polymethyl substitution on Bp affords a 3,3′,4,4′-tetramethyl Bp solute that exhibits superior prelithiation performance toward SiO_x (the solvent is fixed as DME). Choi et al. [123] examined the compatibility of different solvents with electrode materials that are susceptible to co-intercalation, such as Gr. They showed that the weakly solvating solvents, such as THP and mTHF, can regulate the Li^+ solvation structure, promote desolvation, suppress solvent co-intercalation into Gr (Figure 4c), and thus enable the stable chemical prelithiation.

With the sustaining development of LACSs, more attention is paid to enhancing the reversible capacity and cycling stability of the batteries, and to exploiting the reactions between LACSs and electrode materials to construct stable interfacial layers [126–128]. Li et al. [128] employed LACSs that contain the weakly solvating solvent mTHF (in particular, the Bp-Li-mTHF and Naph-Li-mTHF) for chemical prelithiation in SiO_x, and in situ formed a LiF-rich interphase containing species such as Li_2CO_3 and $ROCO_2Li$ (Figure 4d). Such an interphase improved the interfacial stability, suppressed the continuous electrolyte decomposition, and thereby enhanced the cycling performance of the $SiO_x||Li_{1.14}Ni_{0.13}Mn_{0.13}Co_{0.54}O_2$ (LR114) cell (Figure 4e).

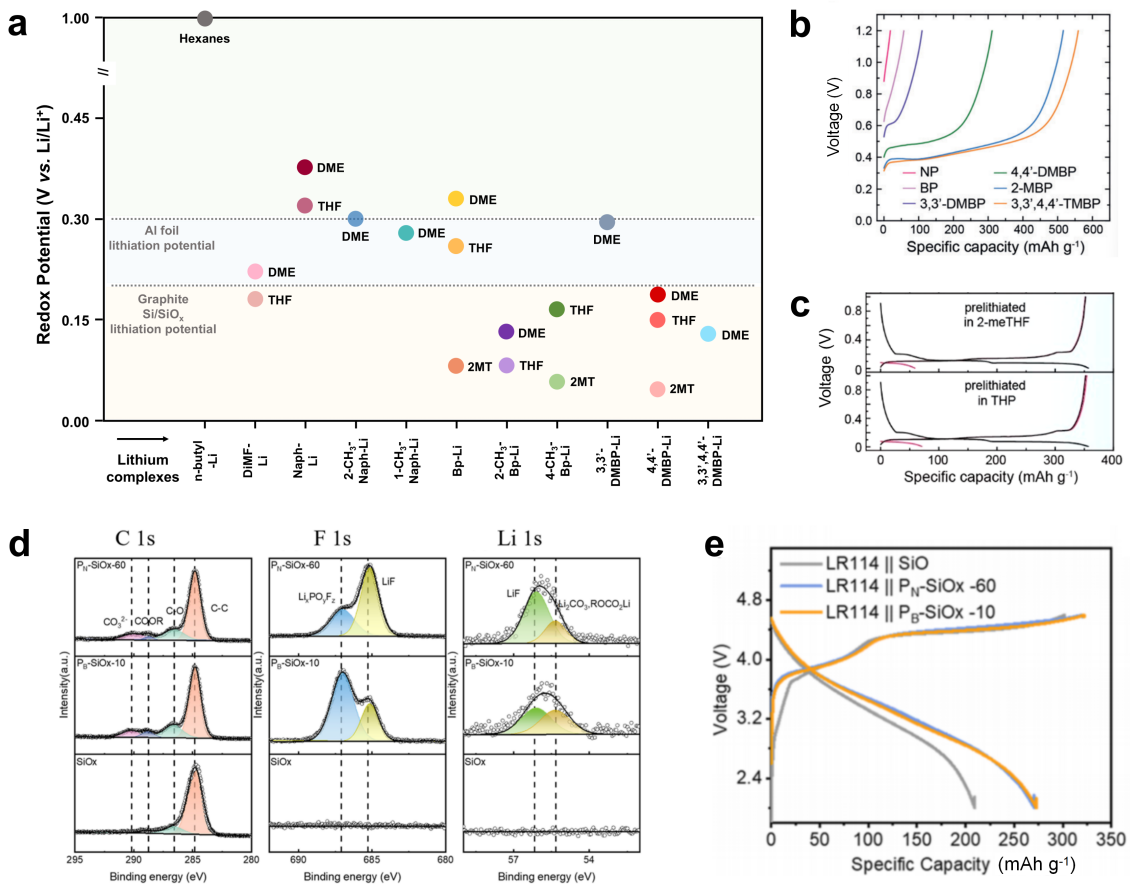

Figure 4. (**a**) The summary of the redox potentials of different LACSs. (**b**) Electrochemical titration of active Li stored in SiO_x electrodes after prelithiation by different LACSs [122]. Reprinted with permission from Ref. [122]. 2020, Jang et al. (**c**) The electrochemical performance of prelithiated Gr by different LACSs in the initial three cycles [123]. (**d**) XPS spectra of C_{1s}, F_{1s}, and Li_{1s} for the SiO_x electrode before and after prelithiation. (**e**) Initial charge/discharge curves of SiO_x||LR114 full cells with or without prelithiated SiO_x [128]. Reprinted with permission from Ref. [128]. 2023, Li et al.

However, several limitations remain. Firstly, precision of the lithiation is still low. Neither the lithiation rate nor the prelithiation content can be accurately regulated, which may induce irreversible structural transformation of the electrode material (e.g., the conversion of $LiCoO_2$ into Co + Li_2O [124]). Secondly, binder compatibility remains a concern. The basic environment of LACSs may degrade the chemical stability of the binder, thereby deteriorating the mechanical integrity of the electrode or making it difficult to form a homogeneous slurry during electrode fabrication. Thirdly, the lithiation effect is highly sensitive to the processing environment. Due to the high reactivity of LACSs, strict control over moisture and oxygen contents is required during preparation and prelithiation. Fourth, the storage lifetime of LACS remains inherently limited, as the radical-mediated nature of the system leads to gradual deactivation during storage and thus hampers long-term preservation.

3. Some of Our Work

3.1. Feasibility of Prelithiation in $LiFePO_4$

LFP has been widely used in energy-storage batteries owing to its low cost and high structural stability. However, its low theoretical capacity (170 mAh g^{-1}) makes the ICE of the LFP-based batteries lower than those using other cathode materials. This makes Li compensation in LFP more essential than in any other cathode material with higher theoretical capacities. In our previous studies on the phase transition mechanism of LFP during delithiation [129], we found that insertion of some Li in LFP does not damage its structure, and some of the lithium can be deintercalated in the subsequent charge. Therefore, we hereby systematically investigated the feasibility of controlled lithium insertion in LFP and its impact on LFP material and on the LFP-based LIBs.

Electrochemical results showed that the initial charge capacity increased markedly with increasing prelithiation depth (Figure 5a). A prelithiation capacity of ca. 50 mAh g^{-1} can well balance increased of initial charge capacity and structural stability. The Fe_{2p} binding energy shifts from 711.0 to 710.7 eV after prelithiation

(Figure 5b). Briefly exposing the prelithiated LFP to dry air (relative humidity 0.1%, exposed for 30 min) does not induce noticeable variation in Fe_{2p} binding energy, demonstrating the good air tolerance of the prelithiated LFP.

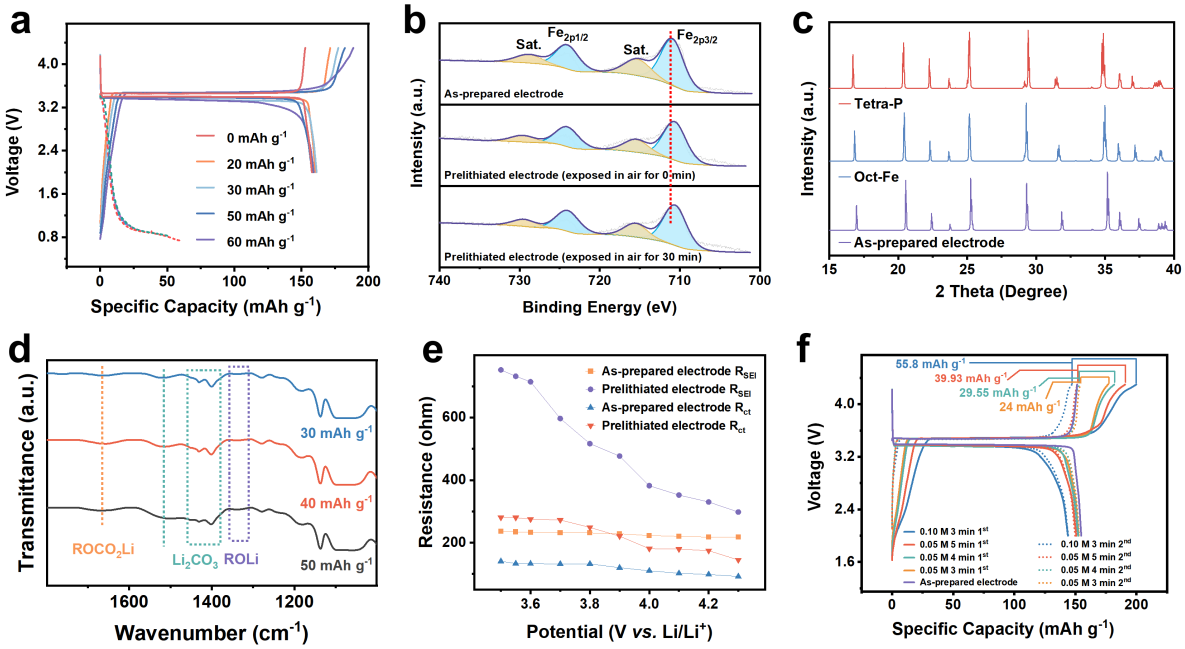

Figure 5. (**a**) The initial discharge/recharge voltage profiles of the LFP electrodes with different prelithiation capacities ($Li_{1+x}FePO_4$, $x \geq 0$). (**b**) The Fe_{2p} binding energy of the LFP electrodes at different states. (**c**) The simulated XRD patterns of the prelithiated LFP with Li occupying different interstitial sites. (**d**) FTIR spectra of the LFP electrodes discharged to different capacities. (**e**) The fitting results of EIS of Li||LFP and Li||$Li_{1+x}FePO_4$ at different voltages. (**f**) The voltage profiles of the chemically prelithiated LFP electrodes in the 1st and 2nd charge-discharge cycles [130]. Reprinted with permission from Ref. [130]. 2022, Cao et al.

Synchrotron X-ray diffraction (XRD) revealed no new phase formation, while density functional theory (DFT) calculations combined with simulated diffraction patterns suggested that the inserted Li preferentially occupies the octahedral Fe site (Oct-Fe) and/or tetrahedral P site (Tetra-P) (Figure 5c). The Fourier-transformed infrared spectra (FTIR, Figure 5d) and electrochemical impedance spectroscopy (EIS, Figure 5e) further revealed that part of the pre-inserted Li was consumed in SEI formation, leading to increased surface-layer and charge-transfer resistance.

Chemical prelithiation was conducted on LFP electrode in Naph-Li-THF solution. Increasing the soaking time or solution concentration enhanced the initial charge capacity, whereas excessive treatment caused over-prelithiation and irreversible conversion of LFP (see the blue line in Figure 5f). Characterization of the prelithiated LFP electrode demonstrates that appropriate chemical prelithiation does not compromise the structural stability of LFP, induce lithiation of Al current collector, or deteriorate the binder properties, as evidenced by the absence of Fe/Li_3PO_4 impurities, the preserved structure and tensile strength of the Al foil, and negligible change in peel strength. These verified the feasibility of LFP prelithiation.

3.2. $Li_xC_6O_6$ as New Organic Additives

Cyclohexanehexone (C_6O_6) was known as a high-capacity electrode material for the Li-ion batteries because each of its six C=O groups can take up one Li^+ ion, corresponding to a theoretical capacity of 957.4 mAh g^{-1} [131]. However, further studies found that C_6O_6 or low Li-content $Li_xC_6O_6$ tends to be dissolved in the usual carbonate electrolyte [132], severely hindering their applications in the current Li-ion batteries. On the other hand, the rapid dissolution of the delithiated $Li_xC_6O_6$ may become an advantage when $Li_xC_6O_6$ is used as a high-efficiency Li compensation additive, as long as the dissolution of C_6O_6 does not bring negative impacts on the solid-state electrolytes and/or the batteries.

We prepared $Li_2C_6O_6$ and $Li_4C_6O_6$ ($Li_xC_6O_6$, x = 2 or 4), respectively, by freeze-drying and sintering as cathode-side Li compensation additives in PEO-based solid-state cells (Figure 6a). The C_{1s} binding energy of the additives remained unchanged after exposure to air (Figure 6b, RH = 20%) for 120 min, demonstrating their high air stability. Electrochemical evaluation indicates that $Li_2C_6O_6$ and $Li_4C_6O_6$ deliver initial capacities of 292.6 and 446.8 mAh g^{-1}, respectively, when charged to 4.2 V but very low Li re-insertion capacities, confirming their

efficient Li donation (Figure 6c). These make them suitable additives in LFP as well as the oxide cathode materials. They boosted the discharge capacity of Cu||LFP full cells from 89.5 to 110.5–122.3 mAh g^{-1} when 5wt% $Li_xC_6O_6$ was added in the LFP cathode (Figure 6d).

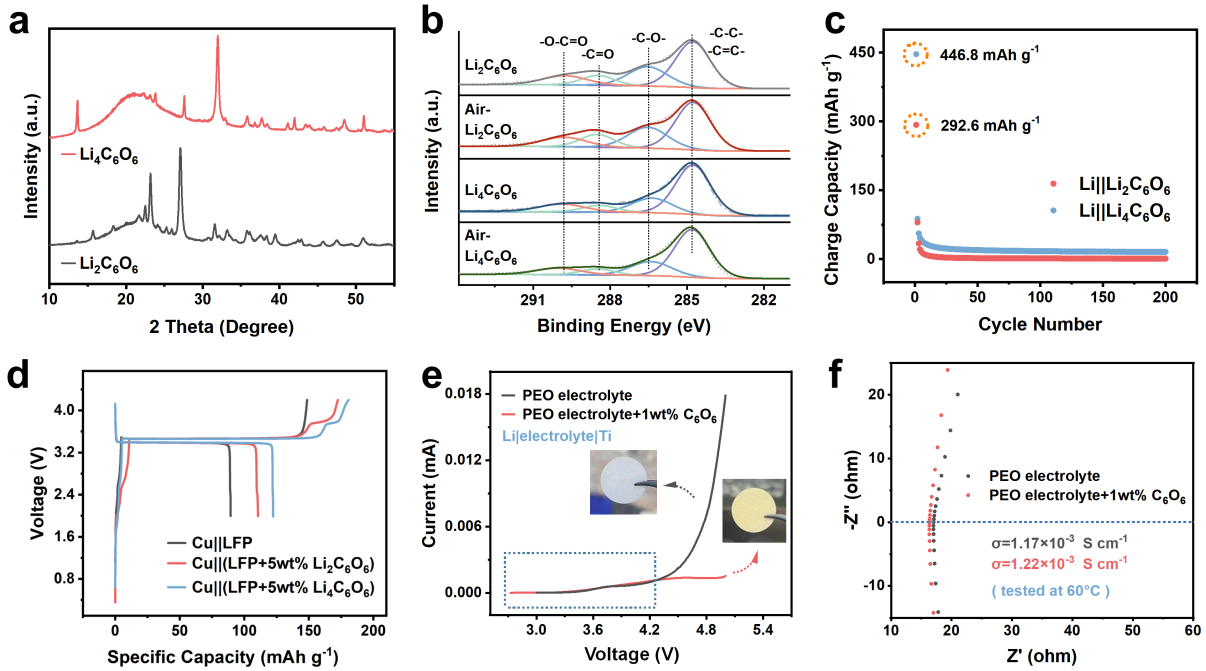

Figure 6. (**a**) XRD patterns of the as-prepared $Li_xC_6O_6$ (x = 2 and 4) powder. (**b**) XPS spectra of C_{1s} for the fresh and air-stored $Li_xC_6O_6$ powder. (**c**) The cycling performance of the $Li_xC_6O_6$ electrode. (**d**) Initial galvanostatic cycling profiles of the Cu||LFP full cells containing 0 wt% or 5 wt% $Li_xC_6O_6$ in the cathode. Comparison of (**e**) the linear sweep voltammetry profiles and (**f**) the impedance spectra of the PEO-based electrolyte with and without 1 wt% C_6O_6 [53].

In addition to the high Li-denotation capacities at low voltages, dissolution of C_6O_6 into either the liquid carbonate electrolyte [133] or PEO-based solid electrolyte does not reduce the electrochemical window (Figure 6e) and the ionic conductivity of the electrolyte (Figure 6f), or alter the glass transition temperature of the PEO electrolyte. These findings not only expand the design space of sacrificial additives beyond conventional inorganic compounds but also open the prospect of developing new and promising cathode sacrificial additives for applications in the battery industry.

3.3. Elucidation of Mechanism of Solution-Based Chemical Prelithiation

Although solution-based chemical prelithiation has progressed rapidly, several obstacles still hinder its commercialization, including degraded air stability of the prelithiated electrodes, limited storage stability of LACSs, and lack of a unified criterion for evaluating prelithiation capability. We conducted a series of studies to respond to these challenges.

Regarding the first challenge, we proposed a two-step solution-treatment strategy to construct an artificial SEI on the prelithiated Gr. By immersing Bp-Li-mTHF-prelithiated Gr (PGr) in different functional solutions, the interphase chemistry was tuned from organic-rich to LiF-rich (Figure 7a). Introduction of artificial SEI markedly improved the storage stability of the PGr electrode in a dry room (relative humidity < 0.3%). In particular, the LiF-rich interphase preserved the lithiated Gr phases (LiC_{12}/LiC_{18}) and achieved an ICE of 129.4%, a capacity of 170 mAh g^{-1} at 3 C, and nearly no obvious decay after 200 cycles at 1C rate. This provides a practical post-prelithiation passivation route for battery manufacturing.

Spectroscopic, gas-evolution, and DFT studies were combined to understand the degradation of LACSs (Figure 7b). It was found that the active monomeric species $Li_1Bp[mTHF]_1$ gradually transformed into a less reactive dimeric species $Li_2Bp[mTHF]_2$, accompanied by the generation of H_2, CH_4, and LiH. The self-metalation of $Li_1Bp[mTHF]_1$ to $Li_2Bp[mTHF]_2$ indicates that $Bp^{\bullet-}$ tends to interact with Li^+ with excess electrons (Figure 7c). Based on this mechanism, we proposed to suppress the disproportionation of $Li_1Bp[mTHF]_1$ and effectively retard

solution degradation by increasing the Bp concentration. When the molar ratio of Li:Bp:mTHF increased from 1.0:1.0:10 to 1.0:1.5:10, the lifetime of the LACS was prolonged to 15 h.

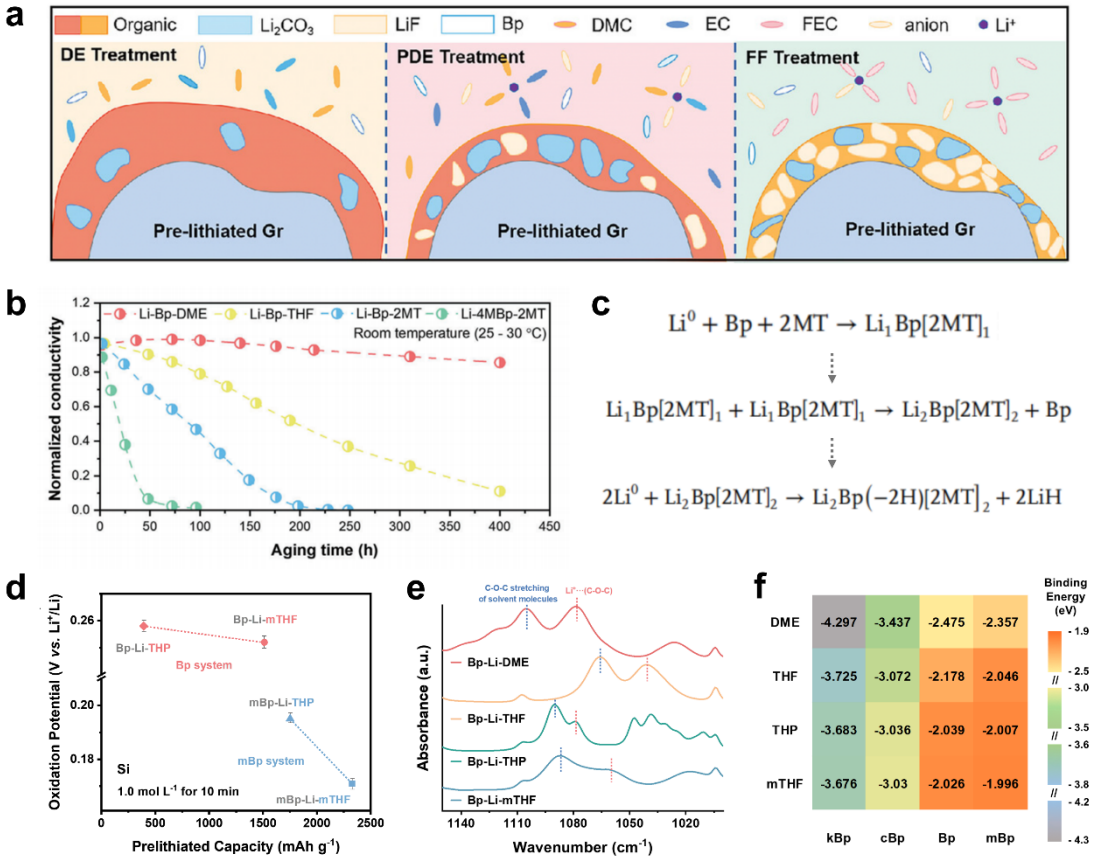

Figure 7. (**a**) Schematic diagram of artificial SEI layers on the solution-treated prelithiated Gr electrodes [134]. Reprinted with permission from Ref. [134]. 2023, Xu et al. (**b**) Evolution of the conductivity of some LACSs with storage (aging) times. (**c**) Supposed degradation pathways of the Bp-Li-mTHF solution [135]. Reprinted with permission from Ref. [135]. 2024, Xu et al. (**d**) Comparison of the prelithiation capabilities of LACSs for the Si anode. (**e**) FTIR spectra of various LACSs. (**f**) The calculated $BE_{solution}$ of Li-ions in different LACSs [136]. Reprinted with permission from Ref. [136]. 2025, Cao et al.

Comparison of the prelithiation behaviors of a series of LACSs containing different aromatic solutes and ether solvents in Si, $Li_4Ti_5O_{12}$, and LFP electrodes indicates that, although the oxidation potential of a LACS (E_O) is correlated with its prelithiation capability, E_O alone cannot well explain the observed prelithiation differences (Figure 7d). As Li^+ desolvation was found the rate-determining step in prelithiation in an electrode material (Figure 7e,f), we proposed the binding-energy-assisted E_O as a descriptor of prelithiation performance of LACS towards a specific electrode material and validated it using a mini database containing 181 solutes and 14 solvents. These findings open the prospect of developing new and promising LACSs for practical applications.

4. Conclusions and Outlooks

Recent years have witnessed rapid advances in Li compensation strategies for high-energy-density LIBs. Electrochemical prelithiation and chemical prelithiation have each shown distinct advantages in compensating the loss of active Li and enhancing the practical energy density of LIBs. These endeavors demonstrate that Li compensation is not merely a supplementary technique for offsetting Li loss but is increasingly becoming an important platform for regulating electrode chemistry, interfacial evolution, and full-cell design.

In comparison, electrochemical prelithiation from the Li-rich compounds and the solution-based chemical prelithiation are more compatible to current manufacturing processes, though compensation by metallic lithium powder and thin foil can be more efficient. Nevertheless, large-scale implementation of additive-based prelithiation still faces several important challenges. For example, the high alkalinity of the Li-rich additives and the prelithiated electrode material make it difficult to prepare uniform slurry or electrode sheets. Meanwhile, the influence of the gas, liquid, and solid residues to the electrolyte, electrode, and even the battery after delithiation

from the additive should also be properly resolved. Therefore, future research should focus on enhancing the utilization of the additives and the storage stability of the electrode material, minimizing side products and residues, and achieving more precise matching between Li release and the operating conditions of commercial batteries. In this context, future efforts may be directed toward the following aspects (Figure 8):

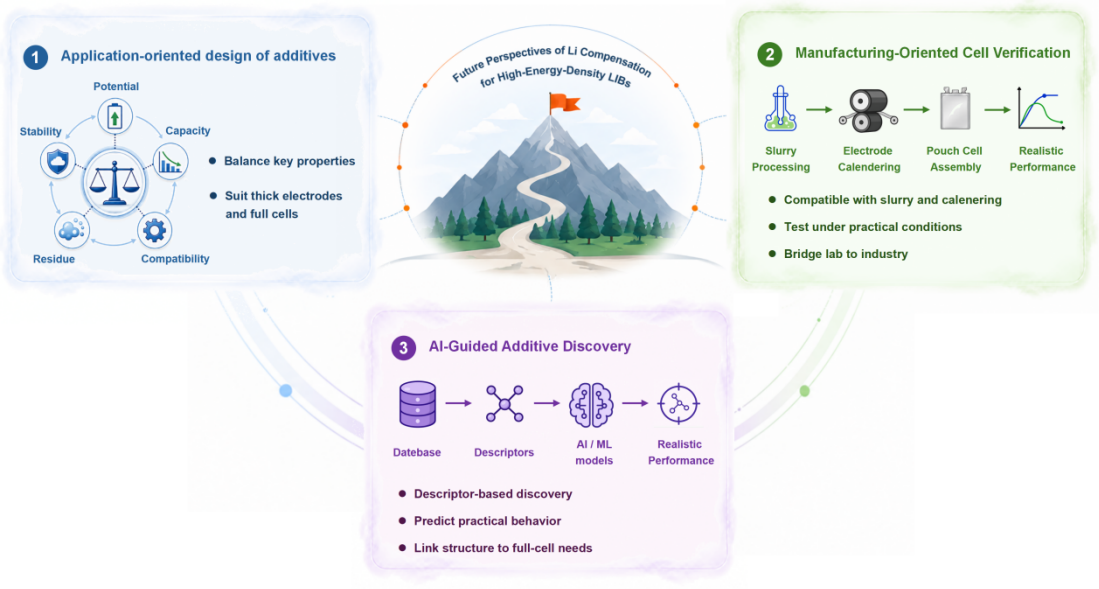

Figure 8. Proposed roadmap for practical Li compensation.

(1) Application-oriented design of additives. Efforts are required to balance delithiation potential, irreversible capacity, air stability, residue/gas generation, and process compatibility of the additives. The matching among Li-compensation amount, release/insertion kinetics, electrode loading, and structural stability, especially in thick electrodes and full-cell configurations, should also be considered.

(2) Verification from material evaluation to battery manufacturing and performance. The value of Li-compensation strategies lies in their compatibility with realistic manufacturing processes, including slurry processing, electrode calendering, moisture tolerance, storage stability, and large-scale fabrication. The Li compensation strategies should be evaluated under application-relevant conditions, such as lean electrolyte, high areal loading, limited Li inventory, pouch-cell formats, and long-term storage, in order to bridge the gap between laboratory demonstration and industrial application.

(3) AI-assisted hunting and performance prediction of Li-compensation additives. Descriptor-based material design can be combined with AI and machine learning to accelerate the search for new Li-compensation additives and to predict their behaviors under practical service conditions. In this way, AI can help bridge fundamental structure-property correlation with realistic full-cell requirements, thereby improving both the efficiency of additive development and the reliability of application-oriented valuation.

Author Contributions

M.C..: conceptualization, investigation, writing-original draft preparation; S.L.: investigation; Y.L.: investigation; Z.W.: supervision, conceptualization, writing-reviewing and editing, funding acquisition; L.C.: writing-reviewing and editing. All authors have read and agreed to the published version of the manuscript.

Funding

This work was financially supported by the National Natural Science Foundation of China (NSFC No. U23A20577).

Institutional Review Board Statement

Not applicable.

Informed Consent Statement

Not applicable.

Data Availability Statement

Date will be made available on request.

Conflicts of Interest

The authors declare no conflict of interest.

Use of AI and AI-Assisted Technologies

No AI tools were utilized for this paper.

References

1. Choi, J.W.; Aurbach, D. Promise and reality of post-lithium-ion batteries with high energy densities. *Nat. Rev. Mater.* **2016**, *1*, 16013.
2. Tan, D.; Meng, Y.; Jang, J. Scaling up high-energy-density sulfidic solid-state batteries: A lab-to-pilot perspective. *Joule* **2022**, *6*, 1755–1769.
3. Chen, Z.-X.; Zhao, M.; Hou, L.-P.; et al. Toward practical high-energy-density lithium-sulfur pouch cells: A review. *Adv. Mater.* **2022**, *34*, 2201555.
4. Peng, M.; Shin, K.; Jiang, L.; et al. Alloy-type anodes for high-performance rechargeable batteries. *Angew. Chem. Int. Ed.* **2022**, *61*, e202206770.
5. Lu, Y.; Yu, L.; Lou, X. Nanostructured conversion-type anode materials for advanced lithium-ion batteries. *Chem* **2018**, *4*, 972–996.
6. Liu, W.; Liu, P.; Mitlin, D. Review of emerging concepts in sei analysis and artificial sei membranes for lithium, sodium, and potassium metal battery anodes. *Adv. Energy Mater.* **2020**, *10*, 2002297.
7. Zhang, H.; Cheng, J.; Liu, H.; et al. Prelithiation: A critical strategy towards practical application of high-energy-density batteries. *Adv. Energy Mater.* **2023**, *13*, 2300466.
8. Jin, L.; Shen, C.; Shellikeri, A.; et al. Progress and perspectives on pre-lithiation technologies for lithium ion capacitors. *Energy Environ. Sci.* **2020**, *13*, 2341–2362.
9. Jin, L.; Shen, C.; Wu, Q.; et al. Pre-lithiation strategies for next-generation practical lithium-ion batteries. *Adv. Sci.* **2021**, *8*, 2005031.
10. Shao, A.; Wang, H.; Zhang, M.; et al. Multiscale interfacial stabilization via prelithiation separator engineering for Ah-level anode-free lithium batteries. *Nat. Commun.* **2025**, *16*, 4145.
11. Meng, Q.; Fan, M.; Chang, X.; et al. A functional prelithiation separator promises sustainable high-energy lithium-ion batteries. *Adv. Energy Mater.* **2023**, *13*, 2300507.
12. Lin, Z.; Tong, Z.; Cai, H.; et al. Prelithiation technology for high energy density lithium-ion batteries: Design, progress, advantages and challenges. *Energy Storage Mater.* **2025**, *83*, 104709.
13. Sun, C.; Zhang, X.; Li, C.; et al. Recent advances in prelithiation materials and approaches for lithium-ion batteries and capacitors. *Energy Storage Mater.* **2020**, *32*, 497–516.
14. Song, Z.; Feng, K.; Zhang, H.; et al. “Giving comes before receiving”: High performance wide temperature range Li-ion battery with $Li_5V_2(PO_4)_3$ as both cathode material and extra Li donor. *Nano Energy* **2019**, *66*, 104175.
15. Aravindan, V.; Satish, R.; Jayaraman, S.; et al. Electrochemical route to alleviate irreversible capacity loss from conversion type α-Fe_2O_3 anodes by $LiVPO_4F$ prelithiation. *ACS Appl. Energy Mater.* **2018**, *1*, 5198–5202.
16. Dose, W.; Kim, S.; Liu, Q.; et al. Dual functionality of over-lithiated NMC for high energy silicon-based lithium-ion batteries. *J. Mater. Chem. A* **2021**, *9*, 12818–12829.
17. Aravindan, V.; Arun, N.; Shubha, N.; et al. Overlithiated $Li_{1+x}Ni_{0.5}Mn_{1.5}O_4$ in all one dimensional architecture with conversion type α-Fe_2O_3: A new approach to eliminate irreversible capacity loss. *Electrochim. Acta* **2016**, *215*, 647–651.
18. Aravindan, V.; Nan, S.; Keppeler, M.; et al. Pre-lithiated $Li_xMn_2O_4$: A new approach to mitigate the irreversible capacity loss in negative electrodes for Li-ion battery. *Electrochim. Acta* **2016**, *208*, 225–230.
19. Aravindan, V.; Ulaganathan, M.; Ling, W.C.; et al. Fabrication of new 2.4 V lithium-ion cell with carbon-coated $LiTi_2(PO_4)_3$ as the cathode. *ChemElectroChem* **2015**, *2*, 231–235.
20. Vargas, Ó.; Caballero, Á.; Morales, J. Deficiencies of chemically reduced graphene as electrode in full li-ion cells. *Electrochim. Acta* **2015**, *165*, 365–371.
21. Wang, Y.; Wang, R.; Dong, J.; et al. Short-circuit prelithiation via electrodeposited Li enables stable inorganic-rich solid electrolyte interphase and superior cycling stability in graphite anodes. *J. Energy Storage* **2026**, *153*, 121056.
22. Niu, X.; Chang, L.; Lu, Y.; et al. A microstructure design-assisted prelithiation method for SiO/Graphite composite anode enabling controllable prelithiation efficiency and homogeneity. *J. Power Sources* **2024**, *613*, 234953.

23. Elazari, R.; Salitra, G.; Gershinsky, G.; et al. Rechargeable lithiated silicon-sulfur (SLS) battery prototypes. *Electrochem. Commun.* **2012**, *14*, 21–24.
24. Zhou, H.; Wang, X.; Chen, D. Li-metal-free prelithiation of SI-based negative electrodes for full li-ion batteries. *ChemSusChem* **2015**, *8*, 2737–2744.
25. Kim, H.J.; Choi, S.; Lee, S.J.; et al. Controlled prelithiation of silicon monoxide for high performance lithium-ion rechargeable full cells. *Nano Lett.* **2016**, *16*, 282–288.
26. An, W.; Gao, B.; Mei, S.; et al. Scalable synthesis of ant-nest-like bulk porous silicon for high-performance lithium-ion battery anodes. *Nat. Commun.* **2019**, *10*, 1447.
27. Li, X.; Liang, J.; Hou, Z.; et al. The design of a high-energy Li-ion battery using germanium-based anode and $LiCoO_2$ cathode. *J. Power Sources* **2015**, *293*, 868–875.
28. Liu, C.; Kim, N.S.; Rubloff, G.W.; et al. High performance asymmetric V_2O_5-SnO_2 nanopore battery by atomic layer deposition. *Nanoscale* **2017**, *9*, 11566–11573.
29. Jayaraman, S.; Aravindan, V.; Ulaganathan, M.; et al. Ultralong durability of porous α-Fe_2O_3 nanofibers in practical Li-ion configuration with $LiMn_2O_4$ cathode. *Adv. Sci.* **2015**, *2*, 1500050.
30. Yu, W.-J.; Zhang, L.; Hou, P.-X.; et al. High reversible lithium storage capacity and structural changes of Fe_2O_3 nanoparticles confined inside carbon nanotubes. *Adv. Energy Mater.* **2016**, *6*, 1501755.
31. Suryawanshi, A.; Aravindan, V.; Mhamane, D.; et al. Excellent performance of Fe_3O_4-perforated graphene composite as promising anode in practical Li-ion configuration with $LiMn_2O_4$. *Energy Storage Mater.* **2015**, *1*, 152–157.
32. Chae, C.; Park, H.; Kim, D.; et al. A Li-ion battery using $LiMn_2O_4$ cathode and MnO_x/C anode. *J. Power Sources* **2013**, *244*, 214–221.
33. Varzi, A.; Bresser, D.; von Zamory, J.; et al. $ZnFe_2O_4$-C/$LiFePO_4$-CNT: A novel high-power lithium-ion battery with excellent cycling performance. *Adv. Energy Mater.* **2014**, *4*, 1400054.
34. Li, Y.; Lv, L.; Liang, R.; et al. Essence of electrochemical prelithiation of the silicon anode: From the interface to the bulk phase. *J. Mater. Chem. A* **2024**, *12*, 20045–20055.
35. Drews, M.; Büttner, J.; Bauer, M.; et al. Spruce hard carbon anodes for lithium-ion batteries. *ChemElectroChem* **2021**, *8*, 4750–4761.
36. Wang, L.; Li, L.; Zhang, X.; et al. Compound-hierarchical-sphere $LiNi_{0.5}Co_{0.2}Mn_{0.3}O_2$: Synthesis, structure, and electrochemical characterization. *ACS Appl. Mater. Interfaces* **2018**, *10*, 32120–32127.
37. Cui, Z.; Zou, F.; Celio, H.; et al. Paving pathways toward long-life graphite/$LiNi_{0.5}Mn_{1.5}O_4$ full cells: Electrochemical and interphasial points of view. *Adv. Funct. Mater.* **2022**, *32*, 2203779.
38. Ha, Y.; Schulze, M.C.; Frisco, S.; et al. Li_2O-based cathode additives enabling prelithiation of SI anodes. *Appl. Sci.* **2021**, *11*, 12027.
39. Sun, Y.; Lee, H.-W.; Seh, Z.W.; et al. High-capacity battery cathode prelithiation to offset initial lithium loss. *Nat. Energy* **2016**, *1*, 15008.
40. Bie, Y.; Yang, J.; Wang, J.; et al. Li_2O_2 as a Cathode additive for the initial anode irreversibility compensation in lithium-ion batteries. *Chem. Commun.* **2017**, *53*, 8324–8327.
41. Zhang, L.; Jeong, S.; Reinsma, N.; et al. Decomposition of Li_2O_2 as the cathode prelithiation additive for lithium-ion batteries without an additional catalyst and the initial performance investigation. *J. Electrochem. Soc.* **2021**, *168*, 120520.
42. Park, K.; Yu, B.-C.; Goodenough, J. Li_3N as a cathode additive for high-energy-density lithium-ion batteries. *Adv. Energy Mater.* **2016**, *6*, 1502534.
43. Sun, Y.; Li, Y.; Sun, J.; et al. Stabilized Li_3N for efficient battery cathode prelithiation. *Energy Storage Mater.* **2017**, *6*, 119–124.
44. Zhu, Y.; Chen, Y.; Chen, J.; et al. Lattice engineering on Li_2CO_3-based sacrificial cathode prelithiation agent for improving the energy density of li-ion battery full-cell. *Adv. Mater.* **2024**, *36*, 2312159.
45. Sun, Y.; Lee, H.-W.; Zheng, G.; et al. In Situ chemical synthesis of lithium fluoride/metal nanocomposite for high capacity prelithiation of cathodes. *Nano Lett.* **2016**, *16*, 1497–1501.
46. Du, J.; Wang, W.; Eng, A.; et al. Metal/LiF/Li_2O nanocomposite for battery cathode prelithiation: Trade-off between capacity and stability. *Nano Lett.* **2020**, *20*, 546–552.
47. Su, X.; Lin, C.; Wang, X.; et al. A new strategy to mitigate the initial capacity loss of lithium ion batteries. *J. Power Sources* **2016**, *324*, 150–157.
48. Liu, C.; Zhang, H.; Zhou, W.; et al. Air-stable Li_5FeO_4 additive enabled by carbon coating for energy-dense lithium-ion batteries. *Nat. Commun.* **2025**, *16*, 7694.
49. Zhu, Y.; Xu, R.; Zheng, Y.; et al. Unravelling the oxygen evolution mechanism of lithium-rich antifluorite prelithiation agent based on anionic oxidation. *Angew. Chem. Int. Ed.* **2025**, *64*, e202502126.
50. Guo, Y.; Li, X.; Wang, Z.; et al. Bifunctional Li_6CoO_4 serving as prelithiation reagent and pseudocapacitive electrode for lithium ion capacitors. *J. Energy Chem.* **2020**, *47*, 38–45.

51. Cui, L.; Li, X.; Wang, Z.; et al. Storage stability of pre-lithiation agent Li_6CoO_4: Exposed to components of dry air and moist gases. *J. Alloys Compd.* **2025**, *1010*, 177976.
52. Liu, G.; Nie, Q.; Wan, W.; et al. Flash upcycling of spent $LiCoO_2$ into oxygen-suppressed lithium-replenishing agent for high-performance batteries. *Nat. Commun.* **2026**, *17*, 41.
53. Cao, M.; Ma, B.; Zhang, S.; et al. Air-stable $Li_2C_6O_6$ and $Li_4C_6O_6$ as high-efficiency lithium compensation additives in cathode. *Energy Mater. Adv.* **2024**, *5*, 0135.
54. Tian, M.; Yan, Y.; Yu, H.; et al. Designer lithium reservoirs for ultralong life lithium batteries for grid storage. *Adv. Mater.* **2024**, *36*, e2400707.
55. Huang, G.; Liang, J.; Zhong, X.; et al. Boosting the capability of $Li_2C_2O_4$ as cathode pre-lithiation additive for lithium-ion batteries. *Nano Res.* **2023**, *16*, 3872–3878.
56. Xia, B.; Zhang, G.; Tao, F.; et al. Promising pre-lithiation agent $Li_2C_2O_4$@KB for high-performance NCM622 cell. *Materials* **2025**, *18*, 4467.
57. Zhang, H.; Bai, T.; Cheng, J.; et al. Unlocking the decomposition limitations of the $Li_2C_2O_4$ for highly efficient cathode preliathiations. *Adv. Powder Mater.* **2024**, *3*, 100215.
58. Xiao, R.; Kang, C.; Ren, Y.; et al. Electrolyte-assisted low-voltage decomposition of $Li_2C_2O_4$ for efficient cathode pre-lithiation in lithium-ion batteries. *Chem. Commun.* **2023**, *59*, 13982.
59. Zhong, W.; Li, S.; Liu, M.; et al. Hierarchical spherical Mo_2C/N-doped graphene catalyst facilitates low-voltage $Li_2C_2O_4$ prelithiation. *Nano Energy* **2023**, *115*, 108757.
60. Niu, Y.-B.; Guo, Y.-J.; Yin, Y.-X.; et al. High-efficiency cathode sodium compensation for sodium-ion batteries. *Adv. Mater.* **2020**, *32*, 2001419.
61. Zhao, J.; Zhou, G.; Yan, K.; et al. Air-stable and freestanding lithium alloy/graphene foil as an alternative to lithium metal anodes. *Nat. Nanotechnol.* **2017**, *12*, 993–999.
62. Zhao, J.; Lee, H.-W.; Sun, J.; et al. Metallurgically lithiated SiO_x anode with high capacity and ambient air compatibility. *Proc. Natl. Acad. Sci. USA* **2016**, *113*, 7408–7413.
63. Wei, H.-X.; Liu, J.-J.; Liu, J.-R.; et al. Carbon-encapsulated Li_2NiO_2 lithium compensator: Decoding failure mechanisms and enabling high-performance pouch cells. *J. Energy Chem.* **2025**, *106*, 387–397.
64. Jia, C.; Shen, Y.-F.; Wang, M.; et al. A high-efficiency pre-lithiation strategy for Li-ion capacitor achieved by the synergistic effect of pre-lithiation and solid electrolyte interface film modification. *J. Energy Storage* **2024**, *99*, 113420.
65. Gu, C.-F.; Chang, X.; Xiao, S.; et al. Element-engineered lithium borate for high-efficiency prelithiation in silicon-based lithium-ion batteries. *Adv. Mater.* **2025**, *37*, e10189.
66. Yan, J.; Wang, L.; Dou, Y.; et al. Anchoring Li_3PO_4 on Li_5FeO_4 surface as a prelithiation additive for lithium-ion batteries. *Langmuir* **2025**, *41*, 26605–26613.
67. Abdullahi, I.L.; Arifiadi, A.; Tsoufios, A.; et al. Lithium squarate as sacrificing electrolyte additive for prelithiation: Case study in zero-excess lithium metal batteries. *Adv. Sci.* **2026**, *13*, e17221.
68. Gomez-Martin, A.; Gnutzmann, M.M.; Adhitama, E.; et al. Opportunities and challenges of $Li_2C_4O_4$ as pre-lithiation additive for the positive electrode in NMC622||Silicon/Graphite lithium ion cells. *Adv. Sci.* **2022**, *9*, 2201742.
69. Wang, D.; Zhang, Z.; Hong, B.; et al. Self-sacrificial organic lithium salt enhanced initial Coulombic efficiency for safer and greener lithium-ion batteries. *Chem. Commun.* **2019**, *55*, 10737–10739.
70. Zhu, B.; Zhang, W.; Li, Z.; et al. "Fe-locking" effect by g-C_3N_4 stabilizing lithium iron oxide pre-lithiation additives. *J. Power Sources* **2024**, *592*, 233944.
71. Sun, Y.; Lee, H.-W.; Seh, Z.W.; et al. Lithium sulfide/metal nanocomposite as a high-capacity cathode prelithiation material. *Adv. Energy Mater.* **2016**, *6*, 1600154.
72. Zhan, Y.; Yu, H.; Ben, L.; et al. Using Li_2S to compensate for the loss of active lithium in li-ion batteries. *Electrochim. Acta* **2017**, *255*, 212–219.
73. Ding, R.; Zheng, Y.; Liang, G. Li_2S as a cathode additive to compensate for the irreversible capacity loss of lithium iron phosphate batteries. *Ionics* **2022**, *28*, 1573–1581.
74. Rao, Z.; Wu, J.; He, B.; et al. A Prelithiation separator for compensating the initial capacity loss of lithium-ion batteries. *ACS Appl. Mater. Interfaces* **2021**, *13*, 38194–38201.
75. Fan, M.; Meng, Q.; Chang, X.; et al. In Situ electrochemical regeneration of degraded $LiFePO_4$ electrode with functionalized prelithiation separator. *Adv. Energy Mater.* **2022**, *12*, 2103630.
76. Cheng, Y.; Tang, T.; Guo, X.; et al. Sandwich-structured $Li_2C_2O_4$@rGO nanospheres via spray-drying for high-efficiency lithium replenishment. *Electrochim. Acta* **2026**, *546*, 147795.
77. Chang, X.; Fan, M.; Yuan, B.; et al. Approaching sustainable lithium-ion batteries through voltage-responsive smart prelithiation separator with surface-engineered sacrificial lithium agents. *Angew. Chem. Int. Ed.* **2024**, *63*, e202406557.
78. Yao, N.; Liu, F.; Shao, A.; et al. Upcycling the spent graphite anode into the prelithiation catalyst: A separator strategy toward anode-free cell prototyping. *Adv. Mater.* **2024**, *36*, e2408268.

79. Liu, G.; Wan, W.; Nie, Q.; et al. Controllable long-term lithium replenishment for enhancing energy density and cycle life of lithium-ion batteries. *Energy Environ. Sci.* **2024**, *17*, 1163–1174.
80. Tao, F.; Yao, Z.; Hou, J.; et al. Molecularly engineered Li compensation agent-integrated separator enabling regeneration of degraded $LiFePO_4$. *J. Mater. Chem. A* **2026**, *14*, 12314–12324.
81. Zhao, J.; Lu, Z.; Wang, H.; et al. Artificial solid electrolyte interphase-protected Li_xSi nanoparticles: An efficient and stable prelithiation reagent for lithium-ion batteries. *J. Am. Chem. Soc.* **2015**, *137*, 8372–8375.
82. Zhao, J.; Lu, Z.; Liu, N.; et al. Dry-air-stable lithium silicide-lithium oxide core-shell nanoparticles as high-capacity prelithiation reagents. *Nat. Commun.* **2014**, *5*, 5088.
83. Zhang, Z.; Sun, Z.; Pei, S.; et al. PEO-$Li_{21}Si_5$ as a pre-lithiation and structural protection layer for lithium-ion batteries. *J. Mater. Chem. A* **2024**, *12*, 9756–9765.
84. Zhang, Z.; Zhang, X.; Liu, Y.; et al. Silicon-based all-solid-state batteries operating free from external pressure. *Nat. Commun.* **2025**, *16*, 1013.
85. Zhao, J.; Sun, J.; Pei, A.; et al. A general prelithiation approach for group IV elements and corresponding oxides. *Energy Storage Mater.* **2018**, *10*, 275–281.
86. Zhang, Z.; Li, Y.; Shen, X.; et al. Breaking the vicious spiral to suppress oxygen loss in li-rich oxide cathode materials. *Adv. Mater.* **2025**, *37*, 2505724.
87. Ji, G.; Wang, J.; Liang, Z.; et al. Direct regeneration of degraded lithium-ion battery cathodes with a multifunctional organic lithium salt. *Nat. Commun.* **2023**, *14*, 584.
88. Yin, Y.-C.; Li, C.; Hu, X.; et al. Rapid, direct regeneration of spent $LiCoO_2$ cathodes for li-ion batteries. *ACS Energy Lett.* **2023**, *8*, 3005–3012.
89. Meng, X.; Hao, J.; Cao, H.; et al. Recycling of $LiNi_{1/3}Co_{1/3}Mn_{1/3}O_2$ cathode materials from spent lithium-ion batteries using mechanochemical activation and solid-state sintering. *Waste Manag.* **2019**, *84*, 54–63.
90. Chung, D.J.; Youn, D.; Kim, S.; et al. Dehydrogenation-driven Li metal-free prelithiation for high initial efficiency SiO-based lithium storage materials. *Nano Energy* **2021**, *89*, 106378.
91. Ou, Y.; Zhang, B.; Zhan, R.; et al. A salt-free medium facilitating electrode prelithiation towards fast-charging and high-energy lithium-ion batteries. *Nat. Commun.* **2025**, *16*, 7956.
92. Yang, C.; Ma, H.; Yuan, R.; et al. Roll-to-roll prelithiation of lithium-ion battery anodes by transfer printing. *Nat. Energy* **2023**, *8*, 703–713.
93. Ma, R.; Liu, Y.; He, Y.; et al. Chemical preinsertion of lithium: An approach to improve the intrinsic capacity retention of bulk SI anodes for li-ion batteries. *J. Phys. Chem. Lett.* **2012**, *3*, 3555–3558.
94. Li, Y.; Qian, Y.; Zhou, J.; et al. Molten-LiCl induced thermochemical prelithiation of SiO_x: Regulating the active Si/O ratio for high initial Coulombic efficiency. *Nano Res.* **2021**, *15*, 230–237.
95. Kim, W.-S.; Yoon, W.-Y. Observation of dendritic growth on Li powder anode using optical cell. *Electrochim. Acta* **2004**, *50*, 541–545.
96. Fan, H.; Li, S.; Yu, Y.; et al. Air-stable Li_xAl foil as free-standing electrode with improved electrochemical ductility by shot-peening treatment. *Adv. Funct. Mater.* **2021**, *31*, 2100978.
97. Shellikeri, A.; Watson, V.; Adams, D.; et al. Investigation of pre-lithiation in graphite and hard-carbon anodes using different lithium source structures. *J. Electrochem. Soc.* **2017**, *164*, A3914–A3924.
98. Liu, N.; Hu, L.; McDowell, M.T.; et al. Prelithiated silicon nanowires as an anode for lithium ion batteries. *ACS Nano* **2011**, *5*, 6487–6493.
99. Meng, Q.; Li, G.; Yue, J.; et al. High-performance lithiated SiO_x anode obtained by a controllable and efficient prelithiation strategy. *ACS Appl. Mater. Interfaces* **2019**, *11*, 32062–32068.
100. Xu, H.; Li, S.; Chen, X.; et al. Sn-alloy foil electrode with mechanical prelithiation: Full-cell performance up to 200 cycles. *Adv. Energy Mater.* **2019**, *9*, 1902150.
101. Xu, H.; Li, S.; Zhang, C.; et al. Roll-to-roll prelithiation of Sn foil anode suppresses gassing and enables stable full-cell cycling of lithium ion batteries. *Energy Environ. Sci.* **2019**, *12*, 2991–3000.
102. Yu, Y.; Li, S.; Fan, H.; et al. Optimal annealing of Al foil anode for prelithiation and full-cell cycling in Li-ion battery: The role of grain boundaries in lithiation/delithiation ductility. *Nano Energy* **2020**, *67*, 104274.
103. Fan, H.; Chen, B.; Li, S.; et al. Nanocrystalline Li-Al-Mn-Si foil as reversible Li host: Electronic percolation and electrochemical cycling stability. *Nano Lett.* **2020**, *20*, 896–904.
104. Wang, C.; Yang, F.; Wan, W.; et al. A large-area lithium metal-carbon nanotube film for precise contact prelithiation in lithium-ion batteries. *Energy Environ. Sci.* **2023**, *16*, 4660–4669.
105. Chen, Y.-X.; Huang, B.-H.; Liu, C.-P. Mechanistic insight into the impact of dry-state prelithiated SiO_x thin-film anode toward extremely fast-charging and long-term stability. *Nano Energy* **2024**, *128*, 109916.
106. Adhitama, E.; Brandao, F.; Bembenek, I.; et al. Pre-lithiation of silicon anodes by thermal evaporation of lithium for boosting the energy density of lithium ion cells. *Adv. Funct. Mater.* **2022**, *32*, 2201455.

107. Aravindan, V.; Lee, Y.-S.; Madhavi, S. Best practices for mitigating irreversible capacity loss of negative electrodes in li-ion batteries. *Adv. Energy Mater.* **2017**, *7*, 1602607.
108. Jarvis, C.R.; Lain, M.J.; Gao, Y.; et al. A lithium ion cell containing a non-lithiated cathode. *J. Power Sources* **2005**, *146*, 331–334.
109. Bärmann, P.; Mohrhardt, M.; Frerichs, J.E.; et al. Mechanistic insights into the pre-lithiation of silicon/graphite negative electrodes in “dry state” and after electrolyte addition using passivated lithium metal powder. *Adv. Energy Mater.* **2021**, *11*, 2100925.
110. Wang, L.; Fu, Y.; Battaglia, V.S.; et al. SBR-PVDF based binder for the application of SLMP in graphite anodes. *RSC Adv.* **2013**, *3*, 15022–15027.
111. Heine, J.; Rodehorst, U.; Qi, X.; et al. Using polyisobutylene as a non-fluorinated binder for coated lithium powder (CLiP) electrodes. *Electrochim. Acta* **2014**, *138*, 288–293.
112. Ji, W.; Zhang, X.; Liu, M.; et al. High-performance all-solid-state Li-S batteries enabled by an all-electrochem-active prelithiated Si anode. *Energy Storage Mater.* **2022**, *53*, 613–620.
113. Hu, C.; Zhang, M.; Zhou, W.; et al. Accurate prelithiation of lithium ion battery SiO_x anodes towards improved initial coulombic efficiency. *Chem. Commun.* **2025**, *61*, 1204–1207.
114. Nagata, H.; Kataoka, K. Mechanochemical partial prelithiation of Si reacted with Li_2O for negative electrode material. *ACS Appl. Energy Mater.* **2026**, *9*, 2344–2351.
115. Garcia, B.; Millet, M.; Pereira-Ramos, J.P.; et al. Electrochemical behavior of chemically lithiated $Li_xV_2O_5$ phases ($0.9 \leq x \leq 1.6$). *J. Power Sources* **1999**, *81*, 670–674.
116. Dose, W.M.; Blauwkamp, J.; Piernas-Muñoz, M.J.; et al. Liquid ammonia chemical lithiation: An approach for high-energy and high-voltage Si-graphite|$Li_{1+x}Ni_{0.5}Mn_{1.5}O_4$ Li-Ion batteries. *ACS Appl. Energy Mater.* **2019**, *2*, 5019–5028.
117. Betz, J.; Nowak, L.; Winter, M.; et al. An approach for pre-lithiation of $Li_{1+x}Ni_{0.5}Mn_{1.5}O_4$ cathodes mitigating active lithium loss. *J. Electrochem. Soc.* **2019**, *166*, A3531–A3538.
118. Zeng, Y.; Zhu, M.; Meng, L.; et al. The role of π electrons in the formation of benzene-containing lithium-bonded complexes. *ChemPhysChem* **2011**, *12*, 3584–3590.
119. Zhang, X.; Qu, H.; Ji, W.; et al. An electrode-level prelithiation of SiO anodes with organolithium compounds for lithium-ion batteries. *J. Power Sources* **2020**, *478*, 229067.
120. Shen, Y.; Qian, J.; Yang, H.; et al. Chemically prelithiated hard-carbon anode for high power and high capacity li-ion batteries. *Small* **2020**, *16*, 1907602.
121. Zhang, X.; Qu, H.; Ji, W.; et al. Fast and controllable prelithiation of hard carbon anodes for lithium-ion batteries. *ACS Appl. Mater. Interfaces* **2020**, *12*, 11589–11599.
122. Jang, J.; Kang, I.; Choi, J.; et al. Molecularly tailored lithium-arene complex enables chemical prelithiation of high-capacity lithium-ion battery anodes. *Angew. Chem. Int. Ed.* **2020**, *59*, 14473–14480.
123. Choi, J.; Jeong, H.; Jang, J.; et al. Weakly solvating solution enables chemical prelithiation of graphite-SiO_x anodes for high-energy li-ion batteries. *J. Am. Chem. Soc.* **2021**, *143*, 9169–9176.
124. Liu, X.; Tan, Y.; Wang, W.; et al. Conformal prelithiation nanoshell on $LiCoO_2$ enabling high-energy lithium-ion batteries. *Nano Lett.* **2020**, *20*, 4558–4565.
125. Shen, Y.; Shen, X.; Yang, M.; et al. Achieving desirable initial coulombic efficiencies and full capacity utilization of li-ion batteries by chemical prelithiation of graphite anode. *Adv. Funct. Mater.* **2021**, *31*, 2101181.
126. Chen, S.; Wang, Z.; Wang, L.; et al. Constructing a robust solid-electrolyte interphase layer via chemical prelithiation for high-performance SiO_x anode. *Adv. Energy Sustain. Res.* **2022**, *3*, 2200083.
127. Li, Y.; Qian, Y.; Zhao, Y.; et al. Revealing the interface-rectifying functions of a Li-cyanonaphthalene prelithiation system for SiO electrode. *Sci. Bull.* **2022**, *67*, 636–645.
128. Li, X.; Bian, C.; Zhang, J.; et al. Chemical pre-lithiation of SiO_x anodes with a weakly solvating solution of polycyclic aromatic hydrocarbons for lithium-ion batteries. *ACS Appl. Energy Mater.* **2023**, *6*, 8919–8928.
129. Sharma, N.; Guo, X.; Du, G.; et al. Direct evidence of concurrent solid-solution and two-phase reactions and the nonequilibrium structural evolution of $LiFePO_4$. *J. Am. Chem. Soc.* **2012**, *134*, 7867–7873.
130. Cao, M.; Liu, Z.; Zhang, X.; et al. Feasibility of prelithiation in $LiFePO_4$. *Adv. Funct. Mater.* **2023**, *33*, 2210032.
131. Lu, Y.; Hou, X.; Miao, L.; et al. Cyclohexanehexone with ultrahigh capacity as cathode materials for lithium-ion batteries. *Angew. Chem. Int. Ed.* **2019**, *58*, 7020–7024.
132. Zhao, Q.; Zhu, Z.; Chen, J. Molecular engineering with organic carbonyl electrode materials for advanced stationary and redox flow rechargeable batteries. *Adv. Mater.* **2017**, *29*, 1607007.
133. Cao, M.; Xu, L.; Guo, Y.; et al. Air-stable $Na_{3.5}C_6O_6$ as a sodium compensation additive in cathode of NA-ion batteries. *Small* **2024**, *20*, 2400498.
134. Xu, S.; Fang, Q.; Wu, J.; et al. Interphase engineering enhanced electro-chemical stability of prelithiated anode. *Small* **2024**, *20*, 2305639.

135. Xu, S.; Liu, Y.; Li, Y.; et al. Degradation mechanism and enhanced stability of organolithium for chemical lithiation. *Adv. Energy Mater.* **2025**, *15*, 2402941.
136. Cao, M.; Ma, B.; Li, Y.; et al. Binding energy-assisted oxidation potential as a measure of prelithiation capability. *Angew. Chem. Int. Ed.* **2026**, *65*, e15463.